Giant Quartz-Hematite veins in the Oman Ophiolite: sub-seafloor or obduction origin? Part 2

Ludwik de Doliwa Zieliński, Larryn Diamond

Rock-Water Interaction, Institute of Geological Sciences, University of Bern

UNIVERSITÄT BERN

Motivation

Understanding fluid migration through oceanic crust allows better understanding of VMS (Volcanogenic Massive Sulfide) ore deposits. Giant quartz–hematite veins testifying to major fluid migration occur in the northern Semail Ophiolite, Oman (Fig. 8). They cut through the ophiolite stratigraphy from the gabbros to the upper volcanic units. However, no evidence is available so far regarding their timing and hence possible relevance to VMS processes. Two contrasting genetic models fit the available constraints: 1) syn-volcanic, i.e., during formation of ocean lithosphere near a MOR (Fig.1); or 2) formation during obduction (Fig.2).

Syn-VMS ~96 Ma

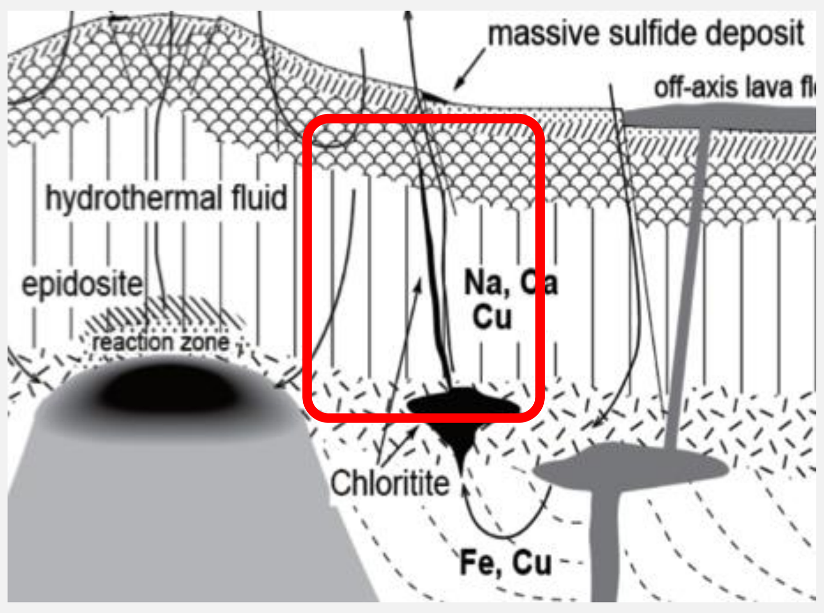

Fig.1 Schematic profile through the oceanic crust, close to MOR. The red square marks the quartz vein system.

Syn-obduction ~70 Ma

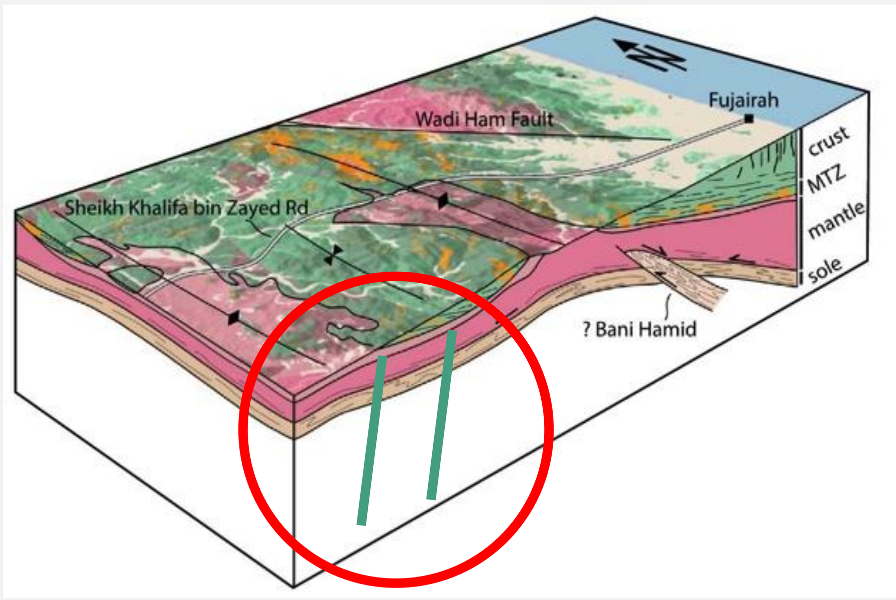

Fig.2 Block profile of obducted Semali ophiolite, this diagram represents the model where the veins (green color) are of syn-obduction origin.

Aims and Methods

To distinguish between the two genetic models we have attempted to determine their timing relative to oceanic magmatism and ophiolite obduction.

Our methods include field mapping and sampling, chlorite thermometry, fluid inclusion thermometry, petrography, EMPA analyses of chlorite and XRF analysis of chlorite-rich alteration haloes.

Vein mineralogy, precipitation sequence

In the field the vein ranges in width from cm scale up to 5 m, and in some cases, it is possible to follow the vein for several kilometres. The vein is surrounded by a chlorite alteration halo that can extend up to 10 m. The vein composition remains similar throughout the stratigraphic sequence: quartz, hematite, chlorite and epidote occur in decreasing order of incidence. The vein paragenesis was defined through petrographic observation (Fig. 3). The relation between quartz and chlorite are complex, as often the chlorite grows in between other minerals, as if it would 'corrode' in. However, some chlorite grains are found as inclusions in other minerals. Inclusion of smaller chlorite and hematite particles in the quartz can be seen (Fig. 5).

Hematite observed in reflected light microscope shows a complex overgrowth pattern (Fig. 4). Using Raman spectroscopy the two phases were identified as hematite and magnetite. The elongated needle like habitus of the mineral indicates hematite as the primary mineral. This process of hematite partially converted to magnetite can by observed in most of the thin section.

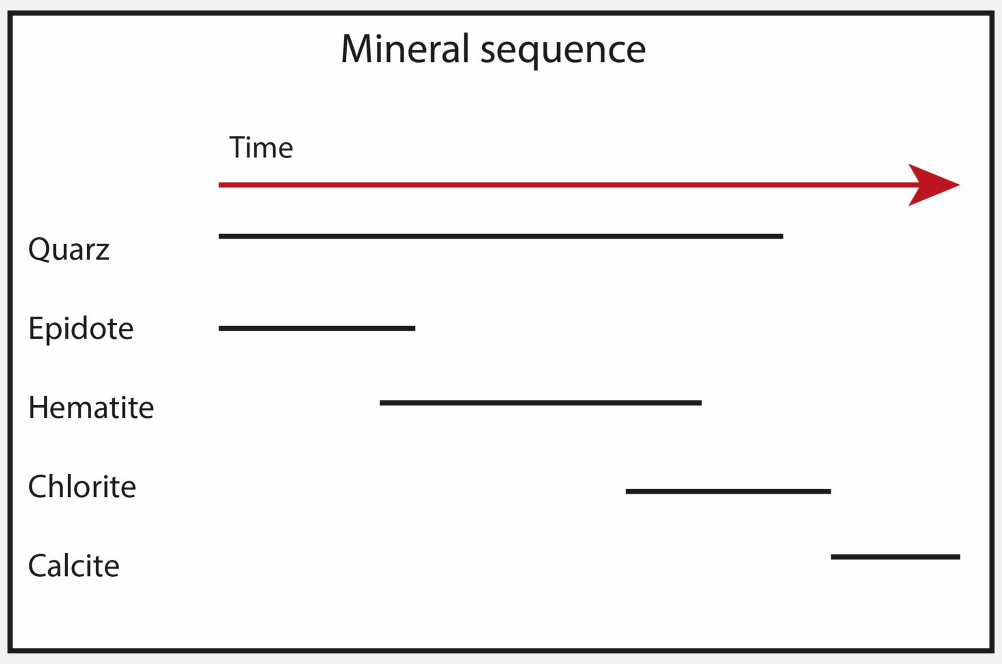

Fig.3

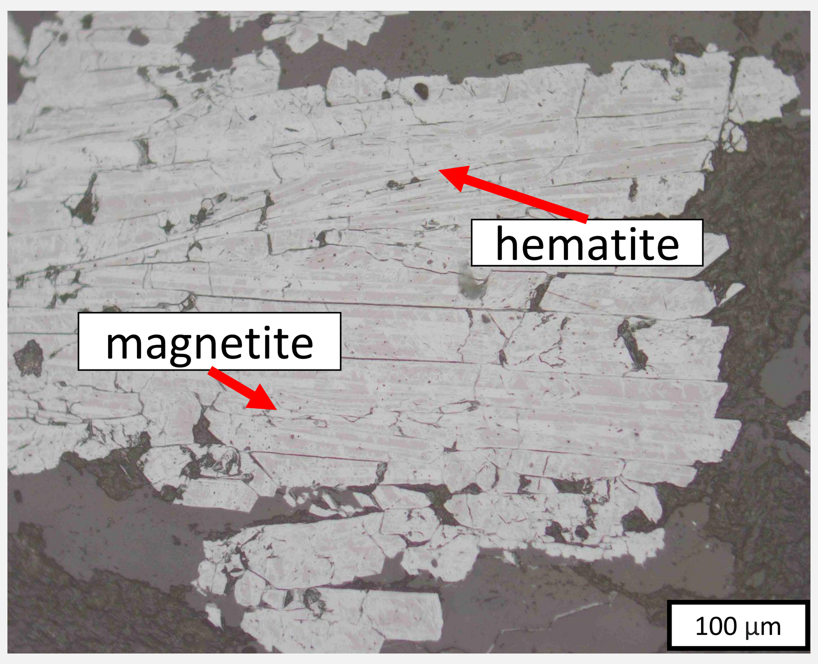

Fig.4 Hematite grain observed under reflected light microscope.

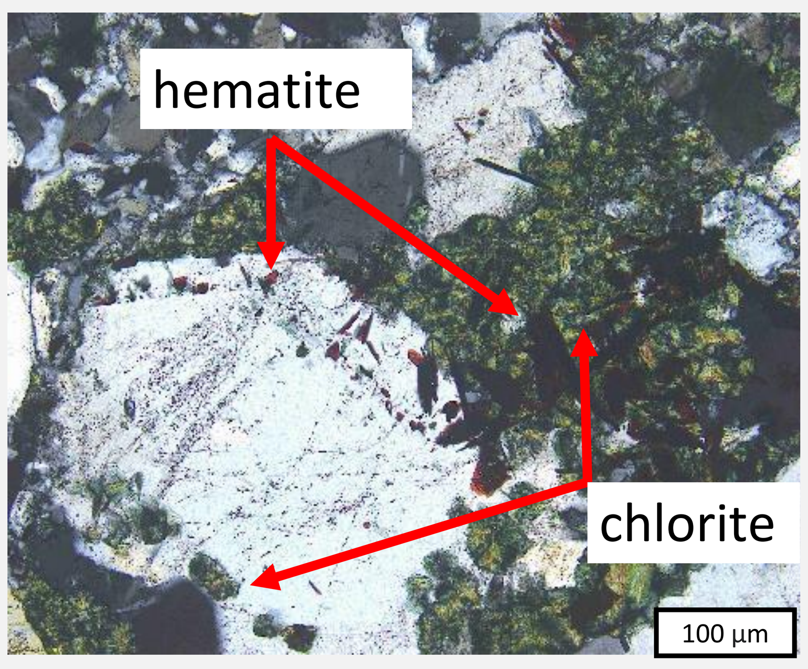

Fig. Quartz, hematite, chlorite vein.

Chlorite thermometry

The chemical composition of chlorite depends on the conditions of formation, such as temperature and pressure, and can be used for thermobarometery (Cathelineau and Nieva 1985,). Additionally, chlorite compositions is also controlled by the bulk rock composition and mineral equilibria (Lanari et al. 2012). There have been different approaches developed for chlorite thermometry. Empirical thermometers are based on the amount of tetrahedral aluminum (Al^{IV}), while semiempirical models are based on the relation between temperature and the equilibrium constant, K. Compared to the thermodynamic approach, the semi-empirical model has a simplified Gibbs free energy equation, activity models and assumptions regarding chlorite Fe3+ content (Vidal et al. 2016). Here, we calculated the temperature with both empirical (Cathelineau 1988; Jowett 1991) and semiempirical models (Inoue et al. 2009, Lanarie 2014).

The Fe^{3+}/Fe_{tot} ratio, which is required in the semiempirical thermometer, was calculated using inverse modelling assuming equilibrium conditions between chlorite endmembers. Therefore, we also observe that their Gibbs free energy was equal (Vidal et al. 2005). The thermometry calculations were done using Matlab, based on the ChlMicaEqui Program from Lanari et al. (2012) and Lanari (2012).

$$T = -61.92 + 321.98\ A1^{IV}$$
(Cathelineau)

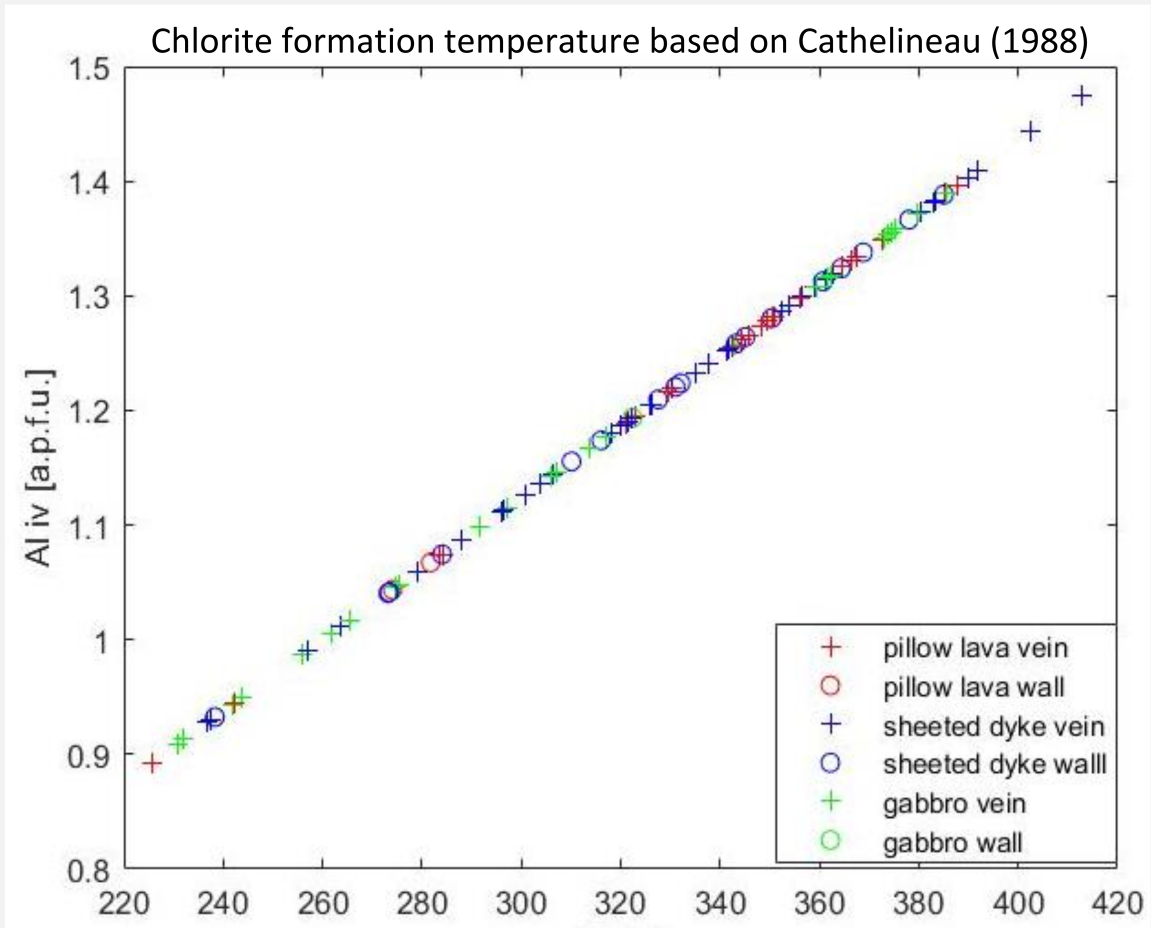

Fig.6

Results

Chlorite formation temperature calculated with the empirical approach, with the thermometer from Cathelineau (1988) is shown in Fig. 6. Fig.7 displays the results from the semiempirical thermometer from Lanari (2014) and Inoue (2009).

It appears that in these veins chlorite formation temperature is not correlated with depth. The calculated T in the samples, collected in the lowest stratigraphic unit, seem to overlap with T calculated for chlorite in the upper lithologies. The two used semiempirical thermometers (Lanari 2014, Inoue 2009) give very similar results. Also the empirical (Cathelineau 1988) and semiempirical thermometers, show simular temperature range for the building of chlorite. There is also no clear difference between chlorites measured in the vein or in the wall rock.

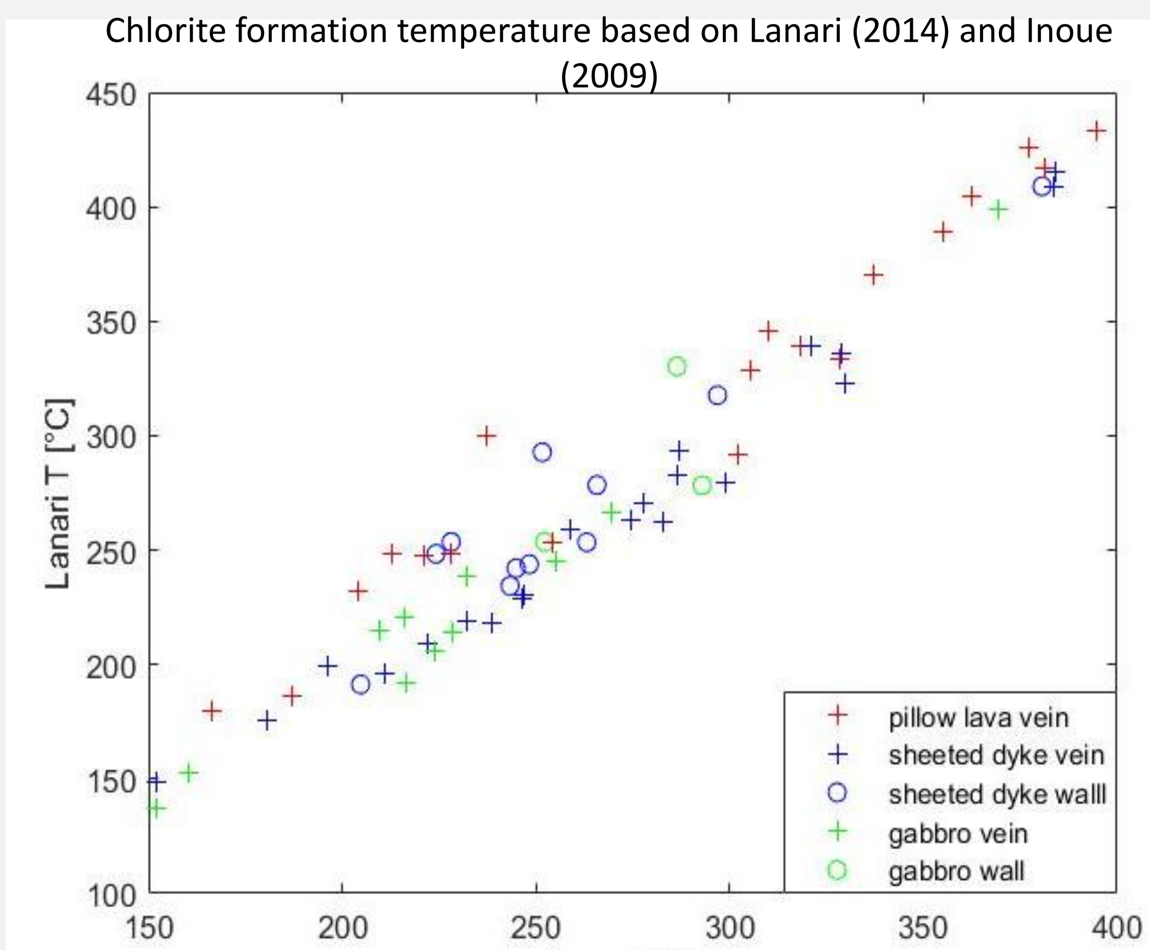

Fig.7

Conclusions

- The veins show uniform textures and mineralogy, regardless of depth.
- The calculated crystallization temperatures of chlorite in the alteration haloes of the veins do not correlate with depth.
- These findings are inconsistent with vein formation in hot oceanic crust during magmatism (Fig. 1), but they are consistent with vein formation after significant cooling of the crust and probably after the syn-obduction warping of the ophiolite into its current anticlinal structure.
- Our results support the syn-obduction model (Fig. 2).

Future Work

- XRD measurements of chlorite across the alteration haloes, to refine chlorite geothermometry.
- SEM nvestigation of the hematite-magnetite overgrowth texture.

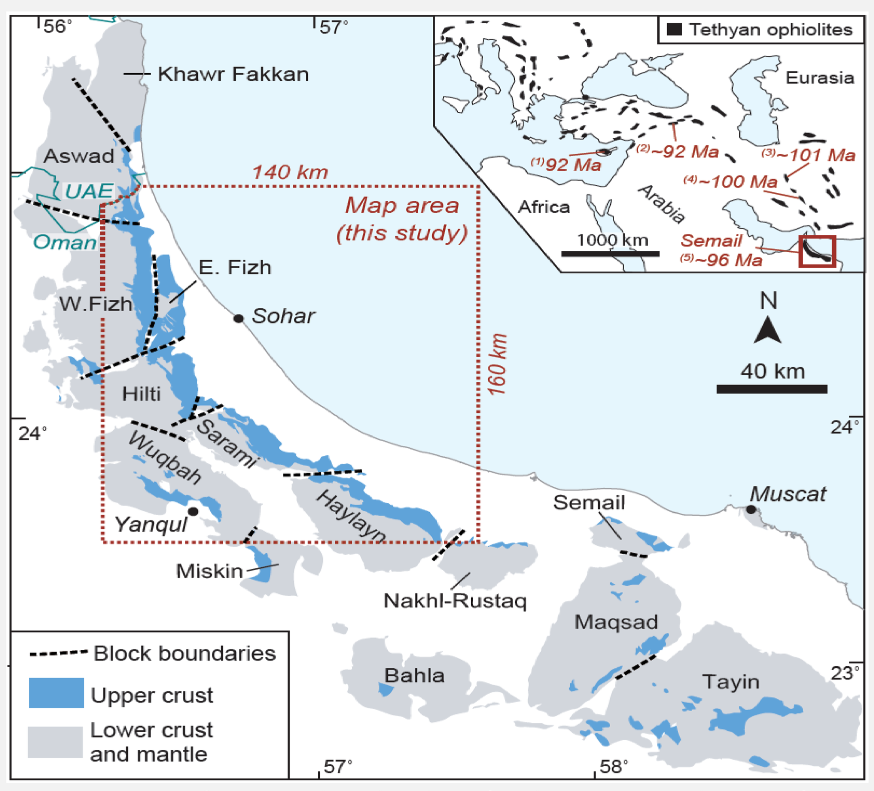

Fig.8 Map of Semail ophiolite (Belgrano et al. 2019)

Fig.9 Quartz vein cutting gabbro.

References

Thomas M. Belgrano, Larryn W. Diamond. Subduction-zone contributions to axial volcanism in the Oman–U.A.E. ophiolite. Lithosphere. 2019, Vol.11, No.3, p.399.

Cathelineau M. (1988) Cation site occupancy in chlorites and illites as function of temperature. *Clay Minerals*, 23, 471–485.

Cathelineau M. & Nieva D. (1985) A chlorite solid solution geothermometer the Los Azufres (Mexico) geothermal system. Contributions to *Mineralogy and Petrology*, 91, 235–244.

Inoue A., Meunier A., Patrier-Mas P., Rigault C., Beaufort D. & Vieillard P. (2009) Application of chemical geothermometry to low-temperature trioctahedral chlorites. *Clays and Clay Minerals*, 57, 371–382.

Jowett E. (1991) Fitting iron and magnesium into the hydrothermal chlorite geothermometer. *Program Abstract*, 16, A62.

Lanari P., Guillot S., Schwartz S., Vidal O., Tricart P., Riel N. & Beyssac O. (2012) Diachronous evolution of the alpine continental subduction wedge: evidence from P-T estimates in the Briançonnais Zone houillère (France—Western Alps). *Journal of Geodynamics*, 56, 39–54.

Lanari P.,Wagner T. & Vidal O. (2014) A thermodynamic model for di-trioctahedral chlorite from experimental and natural data in the system MgO–FeO–Al2O3– SiO2–H2O: applications to P–T sections and geothermometry. *Contributions to Mineralogy and Petrology*, 167, 1–19.

Vidal O., Parra T. & Vieillard P. (2005) Thermodynamic properties of theTschermak solid solution in Fe-chlorite: application to natural examples and possible role of oxidation. *American Mineralogist*, 90, 347–358.

Vidal, O., Lanari, P., Munoz, M., Bourdelle, F., & De Andrade, V. (2016). Deciphering temperature, pressure and oxygen-activity conditions of chlorite formation. *Clay Minerals, 51*(4), 615-633.